

Ultrasound Image Formation in the Deep Learning Age

Muyinatu A. Lediju Bell

John C. Malone Assistant Professor

Department of Electrical and Computer Engineering

Department of Biomedical Engineering

Department of Computer Science

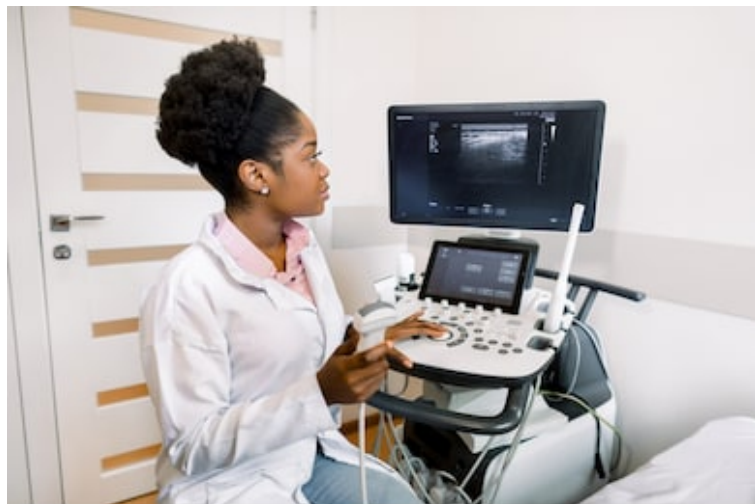


JOHNS HOPKINS
UNIVERSITY



Overview and Historical Perspective

2



shutterstock.com • 1626897577



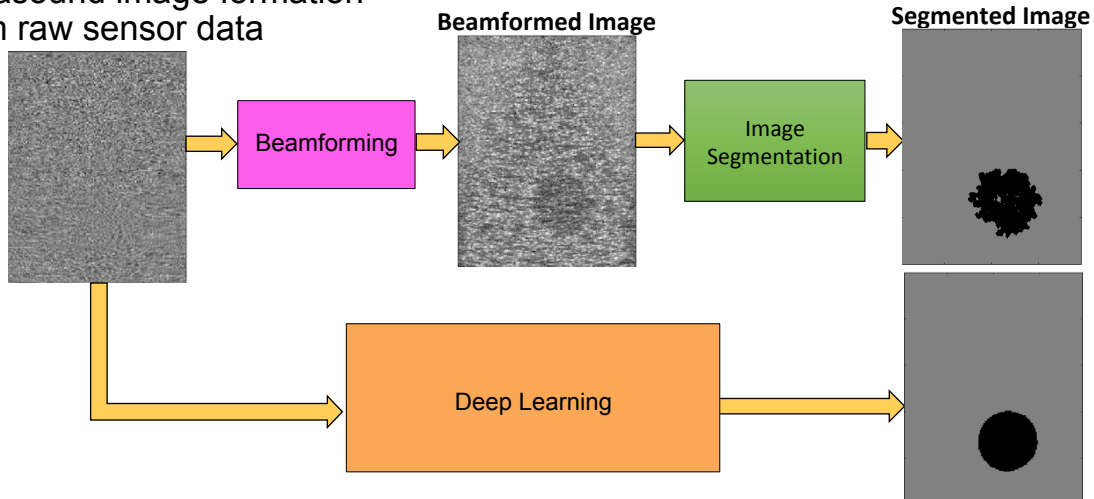
I. Overview II. Point Sources III. Biopsy Targets IV. Speed V. Summary & Outlook



Overview and Historical Perspective

3

- Ultrasound image formation from raw sensor data



I. Overview II. Point Sources III. Biopsy Targets IV. Speed V. Summary & Outlook

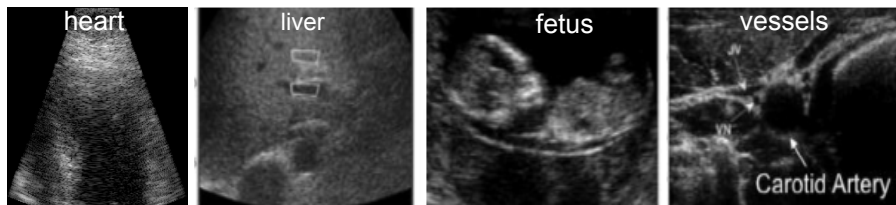


Ultrasound Imaging: Benefits & Challenges

4

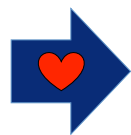
- **Primary benefits:**

- Safe
- Portable
- Real-time
- Cost-effective
- Diagnostic information
- Surgical guidance



- **Outstanding challenges within 60 year history:**

- Noisy
- Speckle
- Acoustic clutter
- Attenuation at depth
- Poor resolution at depth
- Difficult to segment structures
- Difficult to interpret



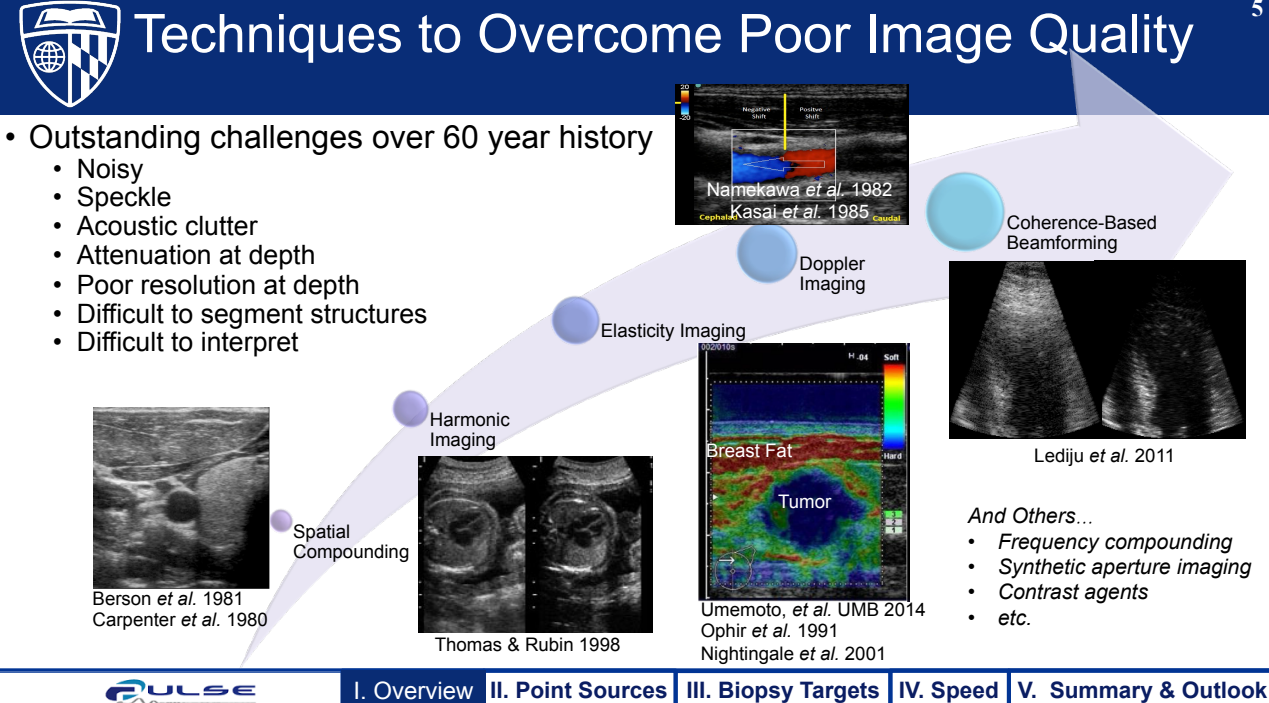
Poor Image Quality



I. Overview II. Point Sources III. Biopsy Targets IV. Speed V. Summary & Outlook

 Techniques to Overcome Poor Image Quality 5

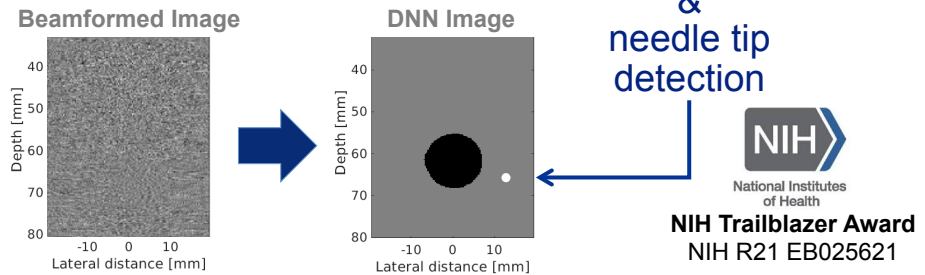
- Outstanding challenges over 60 year history
 - Noisy
 - Speckle
 - Acoustic clutter
 - Attenuation at depth
 - Poor resolution at depth
 - Difficult to segment structures
 - Difficult to interpret



I. Overview II. Point Sources III. Biopsy Targets IV. Speed V. Summary & Outlook

 Deep Learning As Single Solution to Multiple Challenges 6

- Transform noisy, poor contrast images into desired image that only displays structures of interest
- Example:** Deep neural networks (DNNs) to improve **segmentation & needle tip detection**



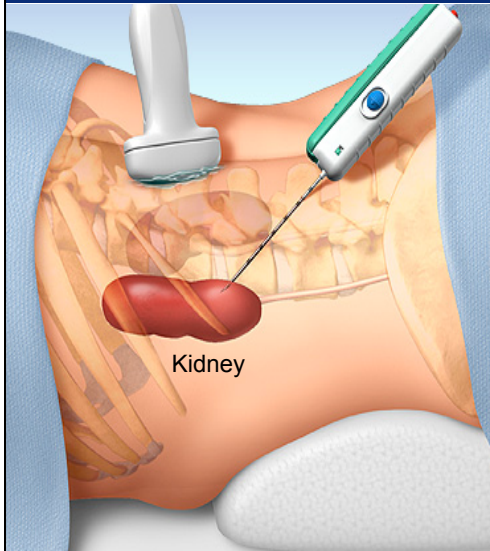
- Significant improvement over current state of the field and overcomes many challenges with poor image quality in single image formation step

I. Overview II. Point Sources III. Biopsy Targets IV. Speed V. Summary & Outlook

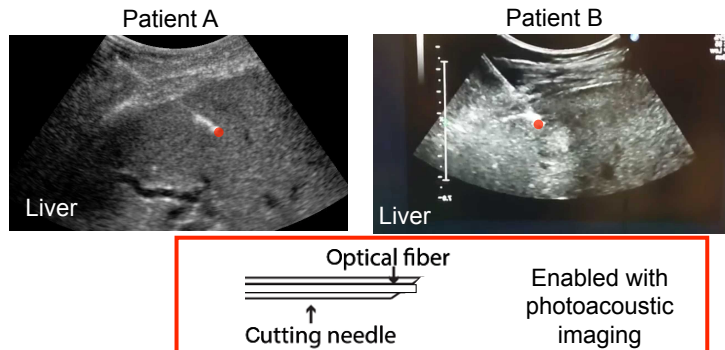


Ultrasound-Guided Biopsy

7



- Small piece of tissue is removed for examination under microscope
- Ultrasound used for needle guidance
- Where is the **needle tip**? Where is the **target**?



PULSE

I. Overview

II. Point Sources

III. Biopsy Targets

IV. Speed

V. Summary & Outlook



Photoacoustic Imaging

8



+



PULSE

I. Overview

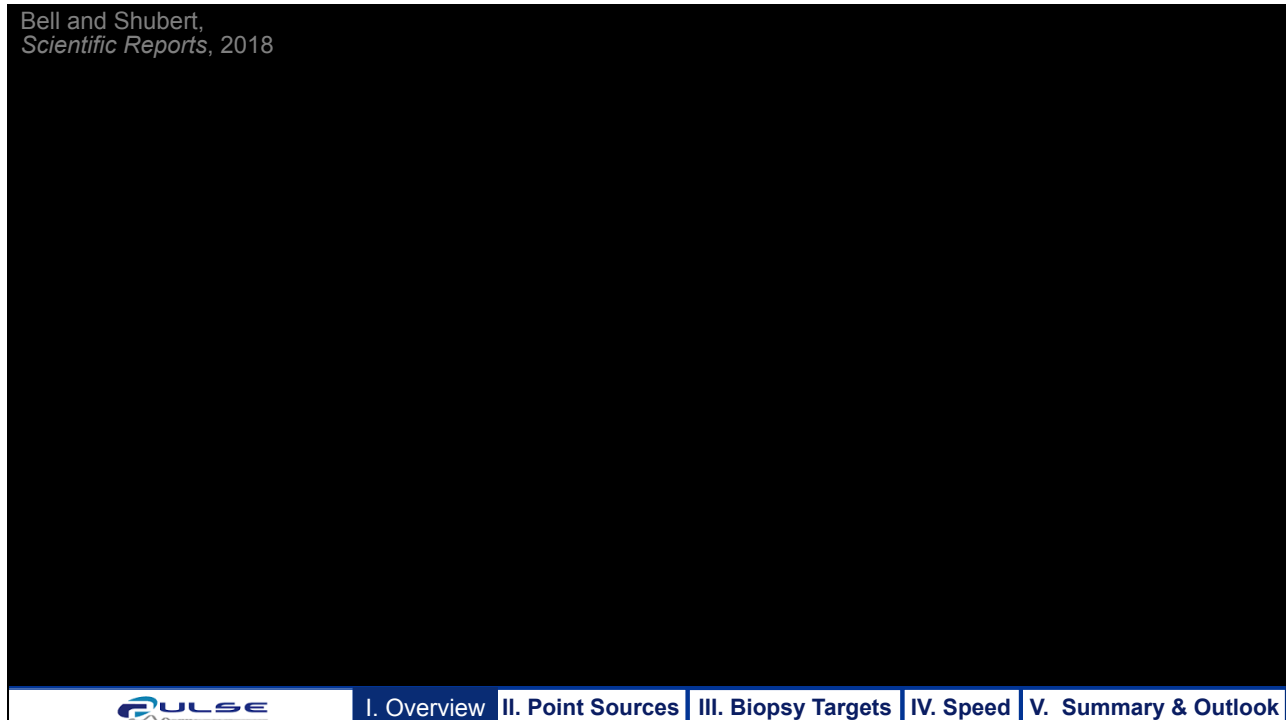
II. Point Sources

III. Biopsy Targets

IV. Speed

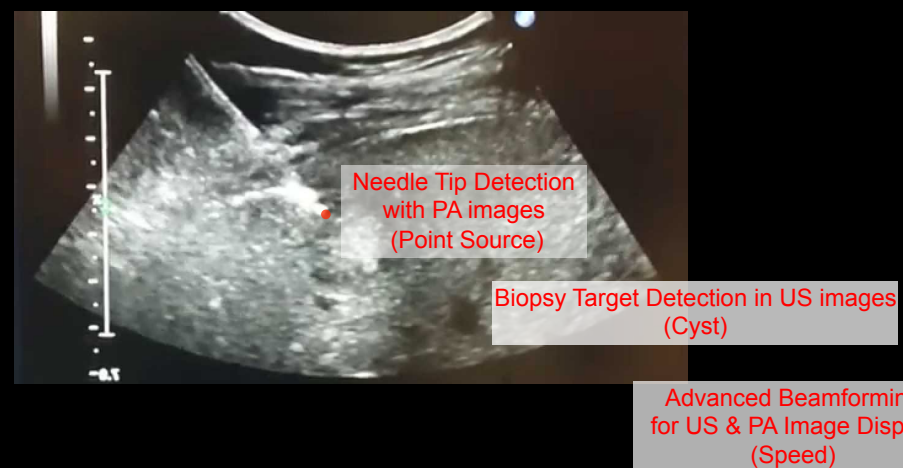
V. Summary & Outlook

Bell and Shubert,
Scientific Reports, 2018

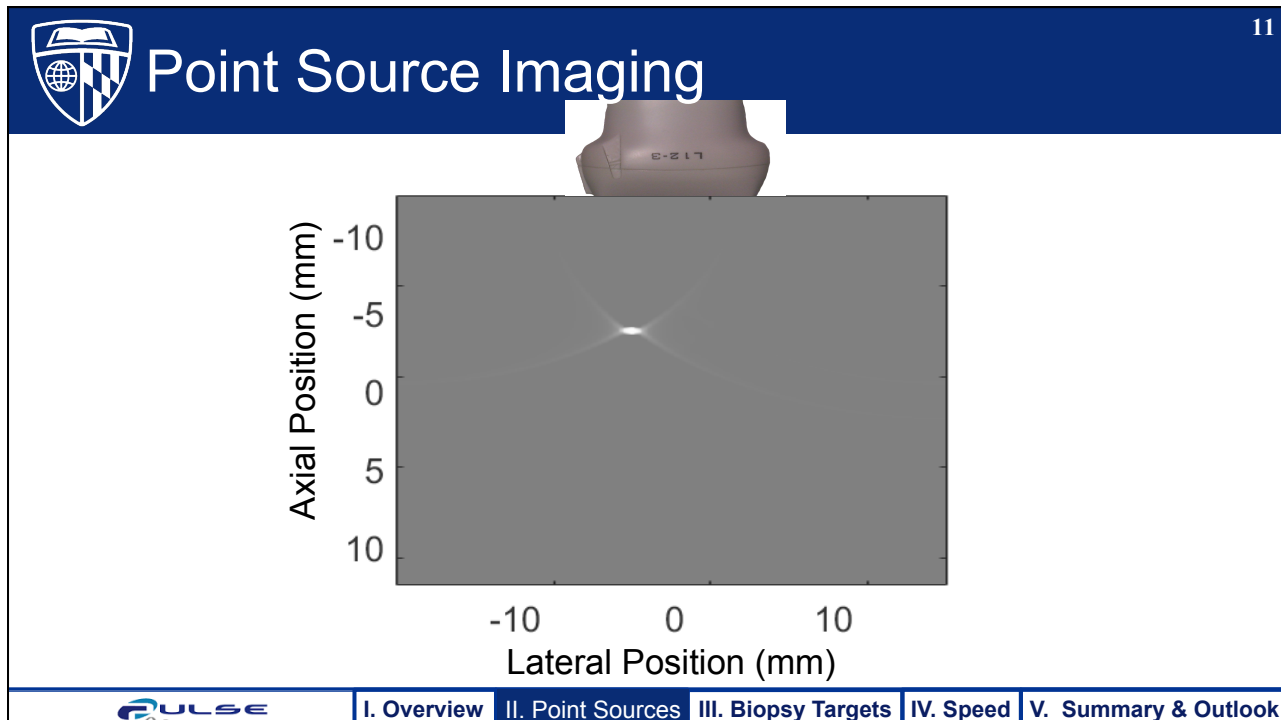


I. Overview II. Point Sources III. Biopsy Targets IV. Speed V. Summary & Outlook

Three Automation Tasks



I. Overview II. Point Sources III. Biopsy Targets IV. Speed V. Summary & Outlook

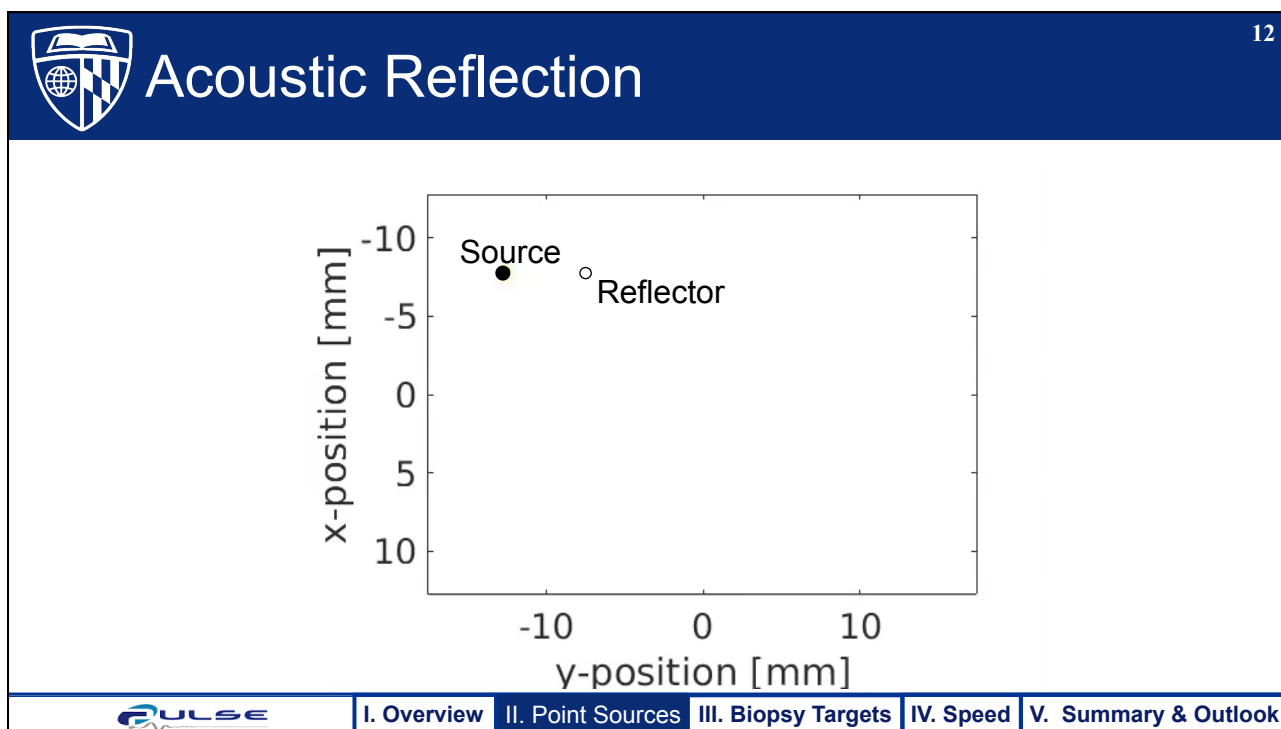


11

Point Source Imaging

A diagram showing a grayscale heatmap of an acoustic field. The horizontal axis is labeled "Lateral Position (mm)" with ticks at -10, 0, and 10. The vertical axis is labeled "Axial Position (mm)" with ticks at -10, -5, 0, 5, and 10. A bright white dot representing the point source is located at approximately (-5, -4). The field shows a characteristic fan-like pattern of decreasing intensity away from the source.

PULSE I. Overview II. Point Sources III. Biopsy Targets IV. Speed V. Summary & Outlook



12

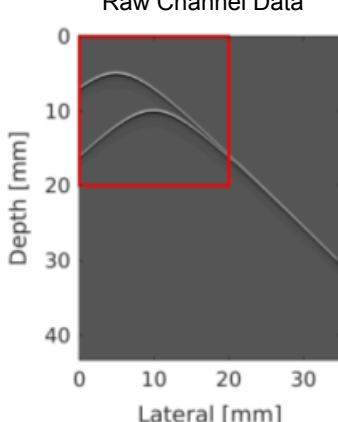
Acoustic Reflection

A diagram illustrating the geometry of an acoustic reflection setup. The horizontal axis is labeled "y-position [mm]" with ticks at -10, 0, and 10. The vertical axis is labeled "x-position [mm]" with ticks at -10, -5, 0, 5, and 10. A solid black dot labeled "Source" is positioned at approximately (-8, -8). An open circle labeled "Reflector" is positioned at approximately (2, -2).

PULSE I. Overview II. Point Sources III. Biopsy Targets IV. Speed V. Summary & Outlook

 **Reflections from Ribs** 13

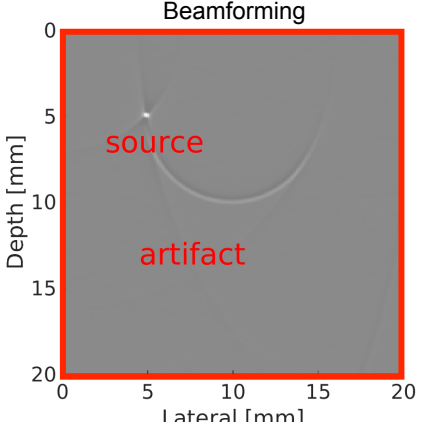
Raw Channel Data



Depth [mm]

Lateral [mm]

After Beamforming



Depth [mm]

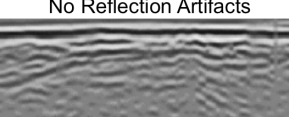
Lateral [mm]

source

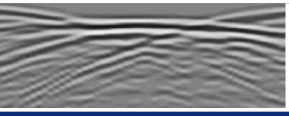
artifact

US Example

Signals with No Reflection Artifacts



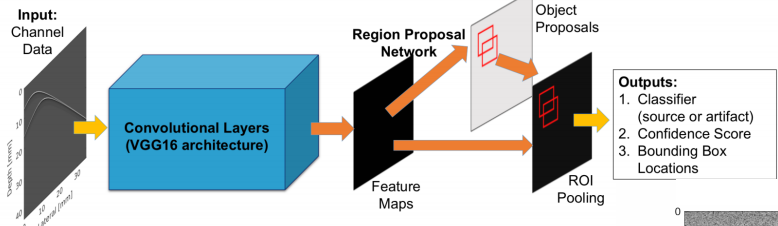
True Signals Mixed with Reflections from Ribs



Artifacts → mapping of signal sources to the wrong location

PULSE
I. Overview
II. Point Sources
III. Biopsy Targets
IV. Speed
V. Summary & Outlook

 **Photoacoustic Source Detection with Deep Learning** 14



Input: Channel Data

Convolutional Layers (VGG16 architecture)

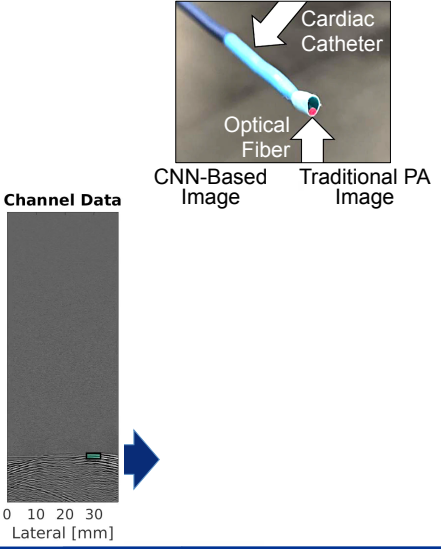
Region Proposal Network

Object Proposals

Outputs:

1. Classifier (source or artifact)
2. Confidence Score
3. Bounding Box Locations

Allman, Reiter, Bell, Photoacoustic Source Detection and Reflection Artifact Removal Enabled by Deep Learning, *IEEE Transactions on Medical Imaging*, 2018



Cardiac Catheter

Optical Fiber

Channel Data

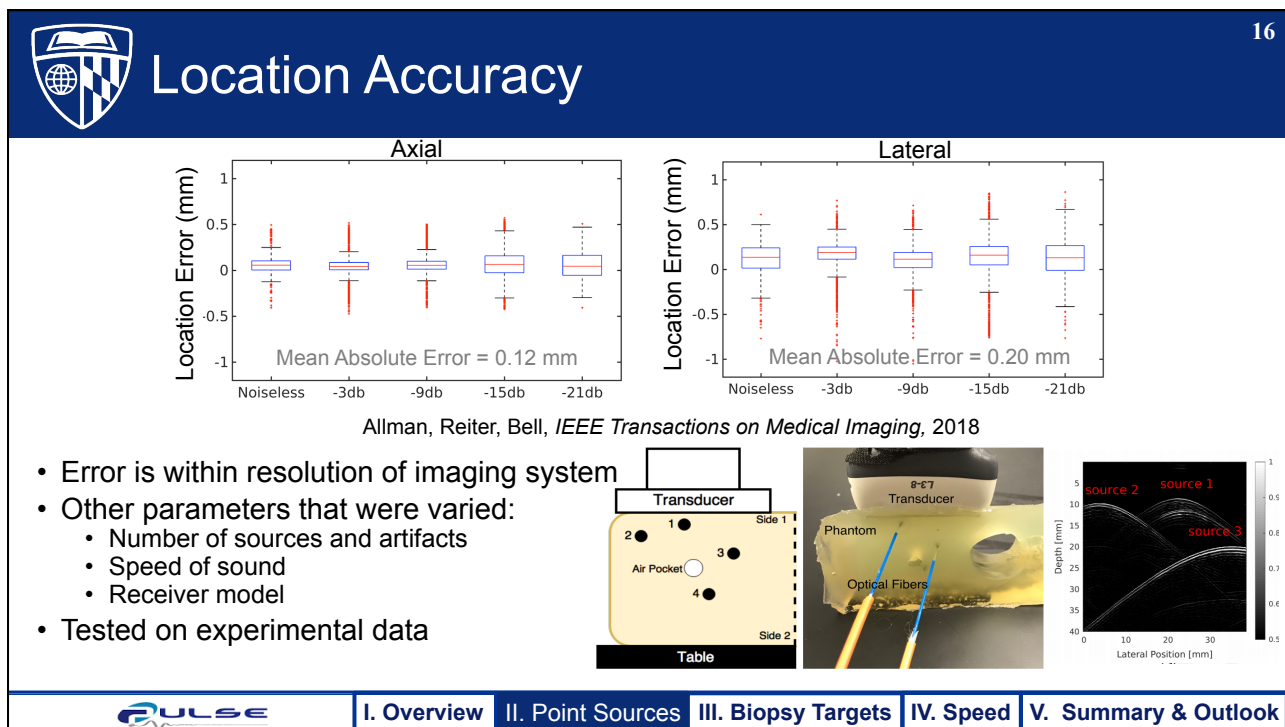
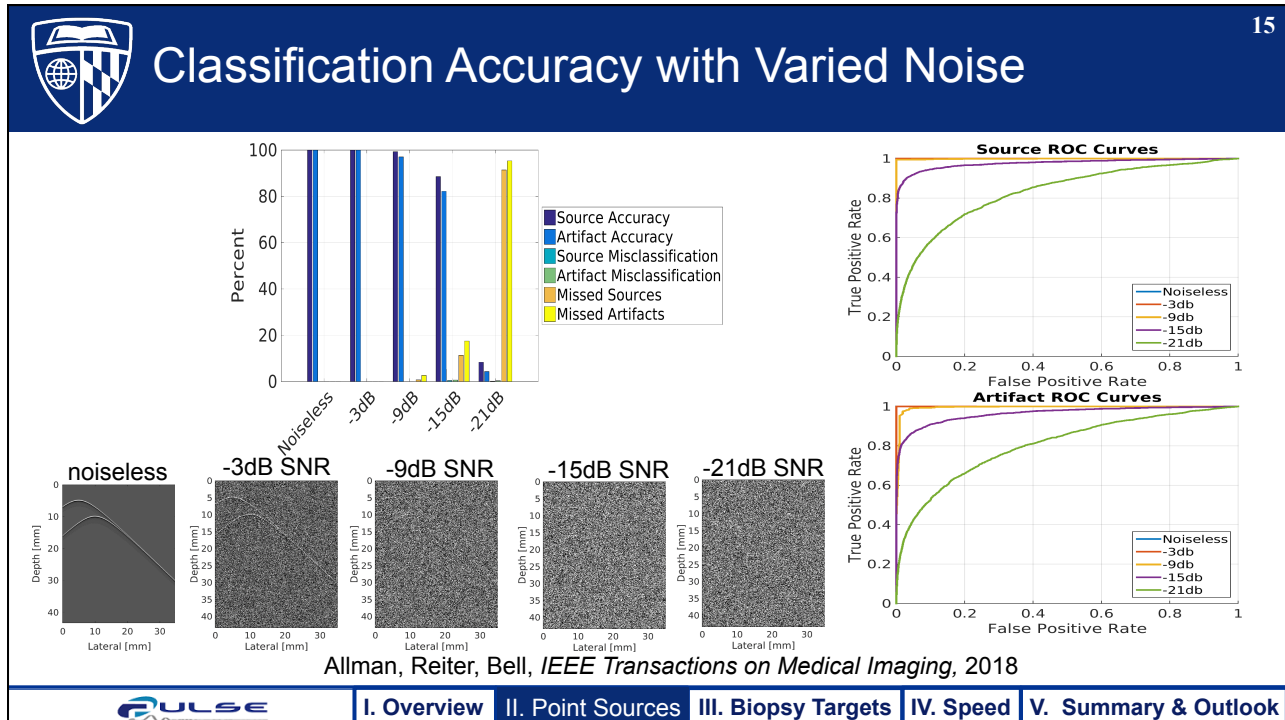
CNN-Based Image

Traditional PA Image

Vein

Example *In Vivo* Result:
Allman, Assis, Chrispin, Bell, Deep neural networks to remove photoacoustic reflection artifacts in *ex vivo* and *in vivo* tissue, *IEEE International Ultrasonics Symposium*, 2018

PULSE
I. Overview
II. Point Sources
III. Biopsy Targets
IV. Speed
V. Summary & Outlook

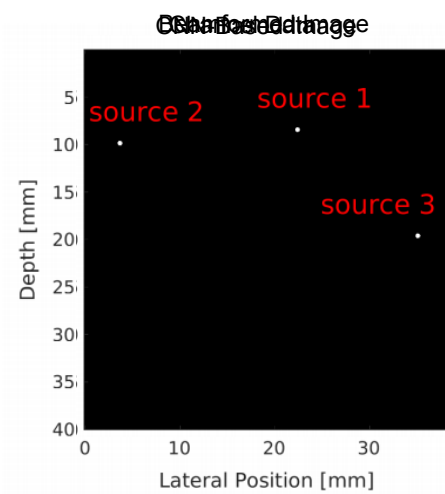




CNN-Based Photoacoustic Image Formation

17

- **Convolutional Neural Network (CNN) enables images with:**
 - No artifacts
 - Arbitrarily high contrast
 - Use network output location along with expected location errors
 - High resolution at depth
 - White region corresponds to $\pm 2\sigma$ of true source location
 - 95% certain that the true source is centered in this region



Allman, Reiter, Bell, *IEEE Transactions on Medical Imaging*, 2018

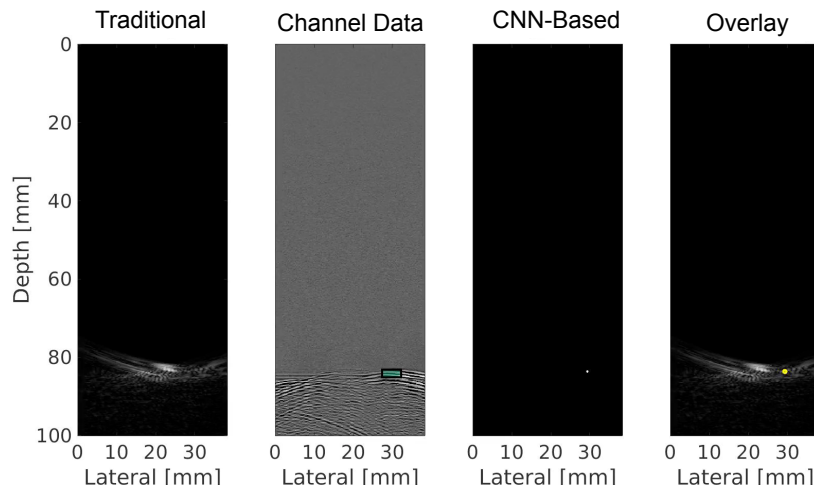
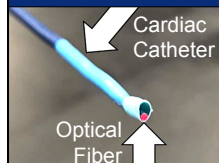


I. Overview II. Point Sources III. Biopsy Targets IV. Speed V. Summary & Outlook



In Vivo Cardiac Catheterization Example

18



Allman D, Assis F, Chrispin J, Bell MAL, Deep neural networks to remove photoacoustic reflection artifacts in ex vivo and in vivo tissue, *IEEE International Ultrasonics Symposium*, 2018



I. Overview II. Point Sources III. Biopsy Targets IV. Speed V. Summary & Outlook



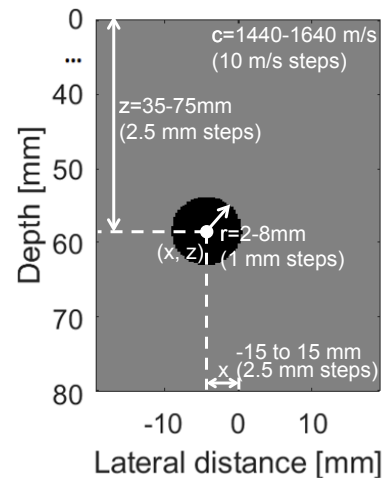
Train with Simulations that Mimic Physics

19

- Single cyst in tissue
 - Anechoic: 32,487 raw RF plane wave data examples
 - Hypoechoic (-6dB contrast): 17,199 raw RF examples
- One plane wave, insonification angle
- Simulation parameters:
 1. Cyst radius (r)
 2. Medium sound speeds (c)
 3. Axial position of cyst center (z)
 4. Lateral position of cyst center (x)
- Simulated test set:
 - 100 additional RF plane wave examples - parameters randomly chosen from within training ranges
 - Contrast randomly chosen between anechoic and -6dB

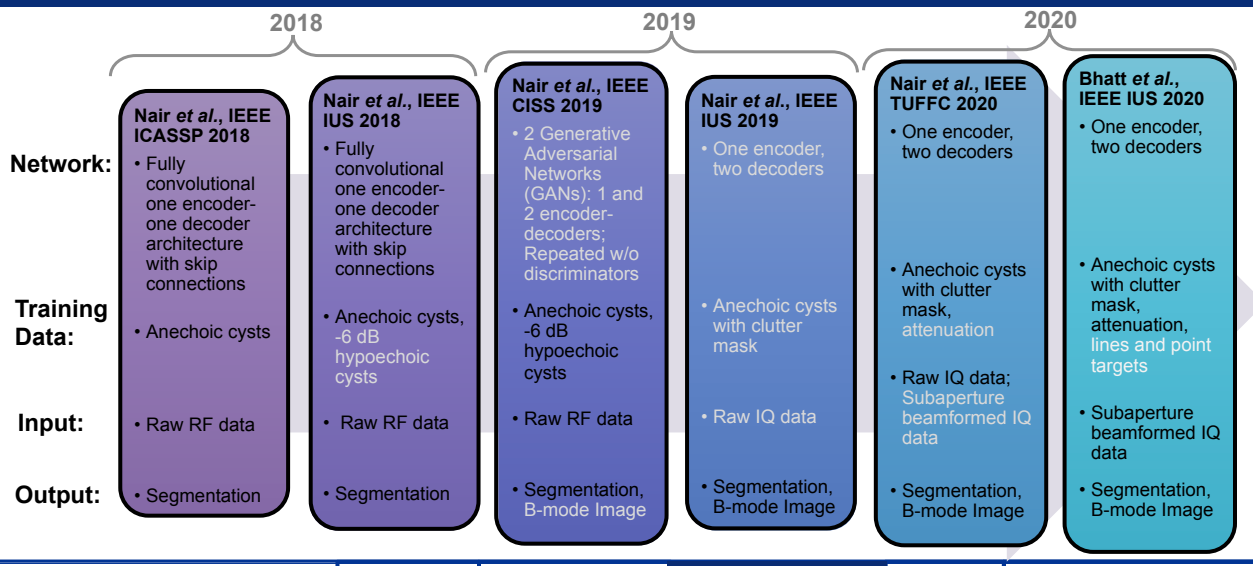
Nair et al. IEEE ICASSP 2018

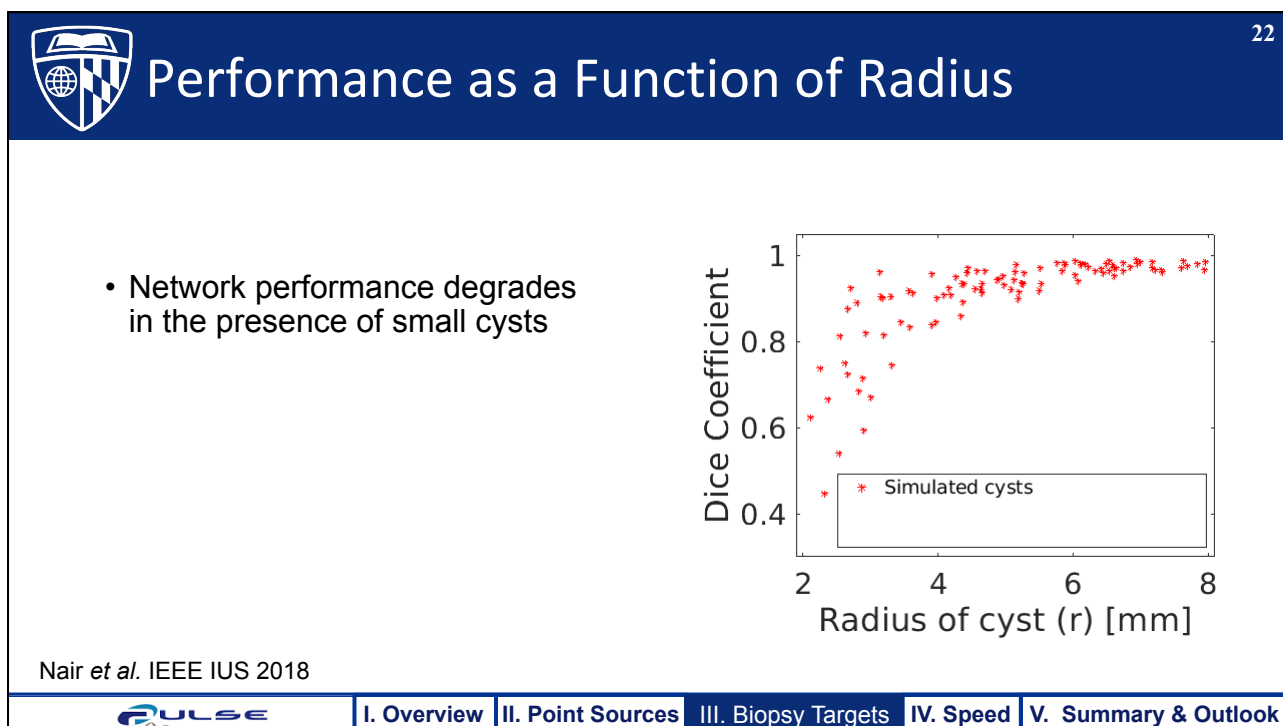
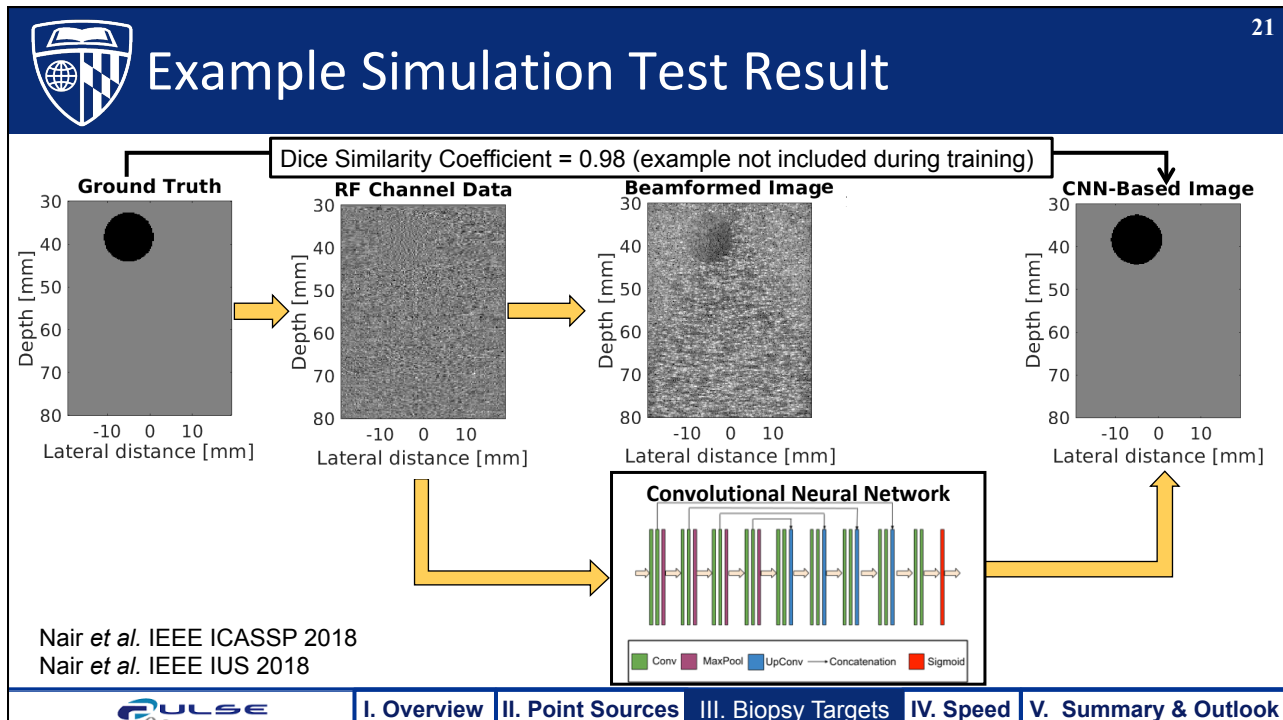
Nair et al. IEEE IUS 2018

**PULSE**
[I. Overview](#) | [II. Point Sources](#) | [III. Biopsy Targets](#) | [IV. Speed](#) | [V. Summary & Outlook](#)


Evolution of US Networks & Training Methods

20

**PULSE**
[I. Overview](#) | [II. Point Sources](#) | [III. Biopsy Targets](#) | [IV. Speed](#) | [V. Summary & Outlook](#)

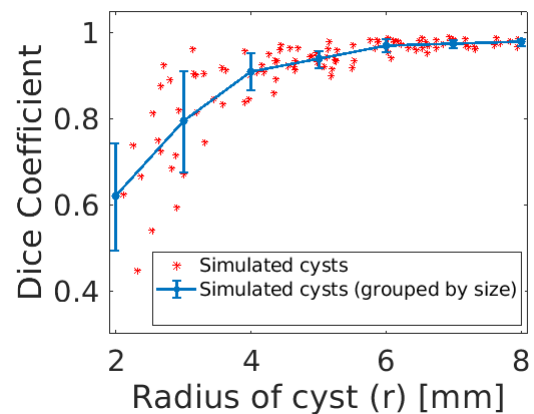




Performance as a Function of Radius

23

- Network performance degrades in the presence of small cysts
- The radius of each simulated cyst was rounded to the nearest integer mm



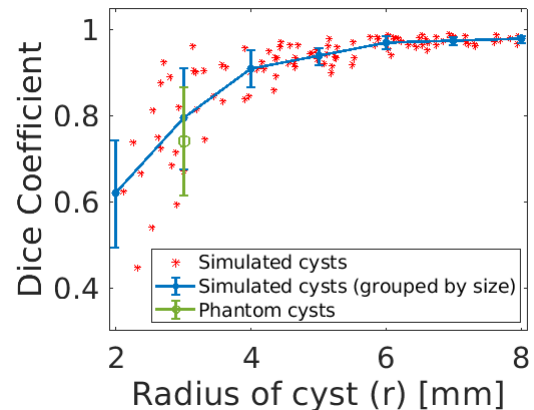
Nair et al. IEEE IUS 2018


[I. Overview](#) [II. Point Sources](#) [III. Biopsy Targets](#) [IV. Speed](#) [V. Summary & Outlook](#)


Performance as a Function of Radius

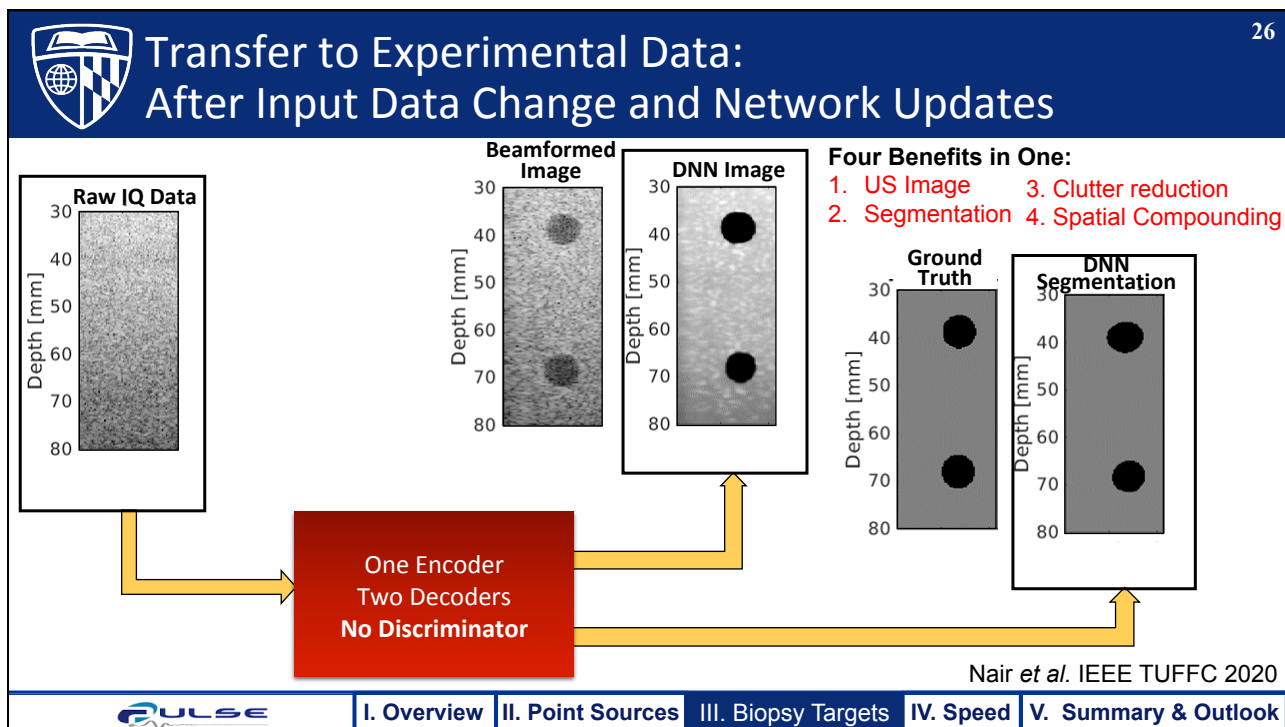
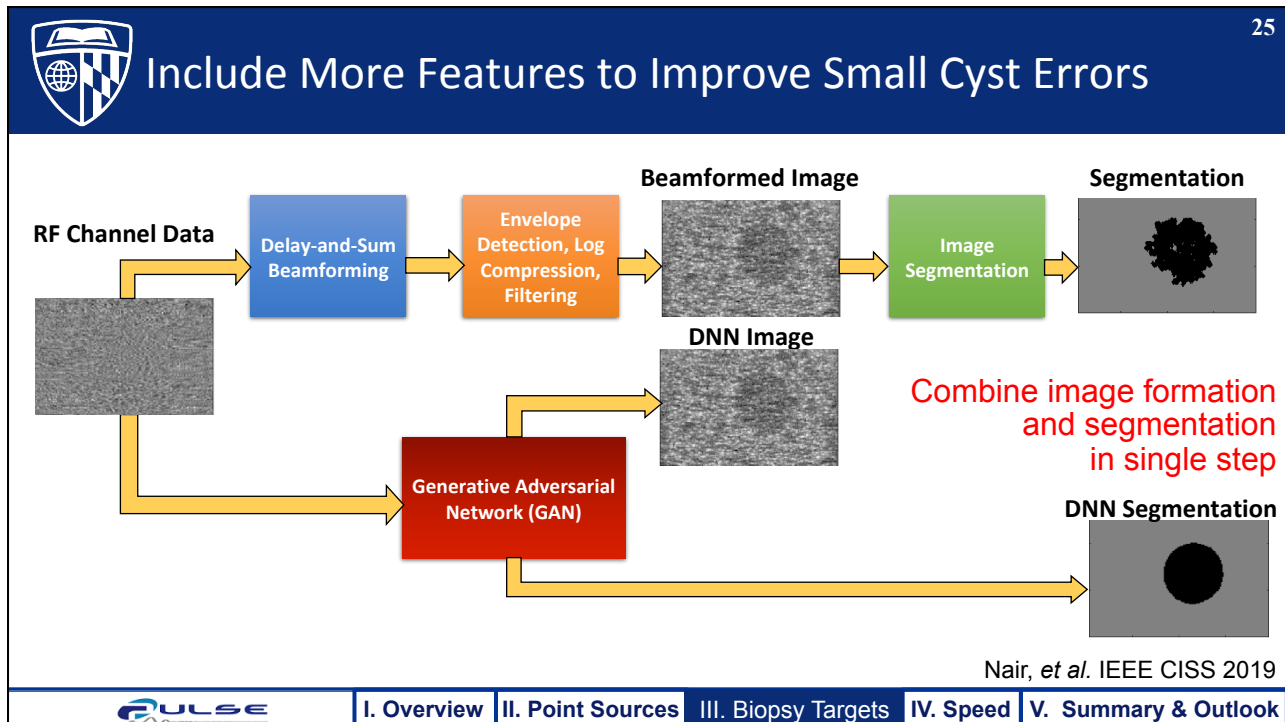
24

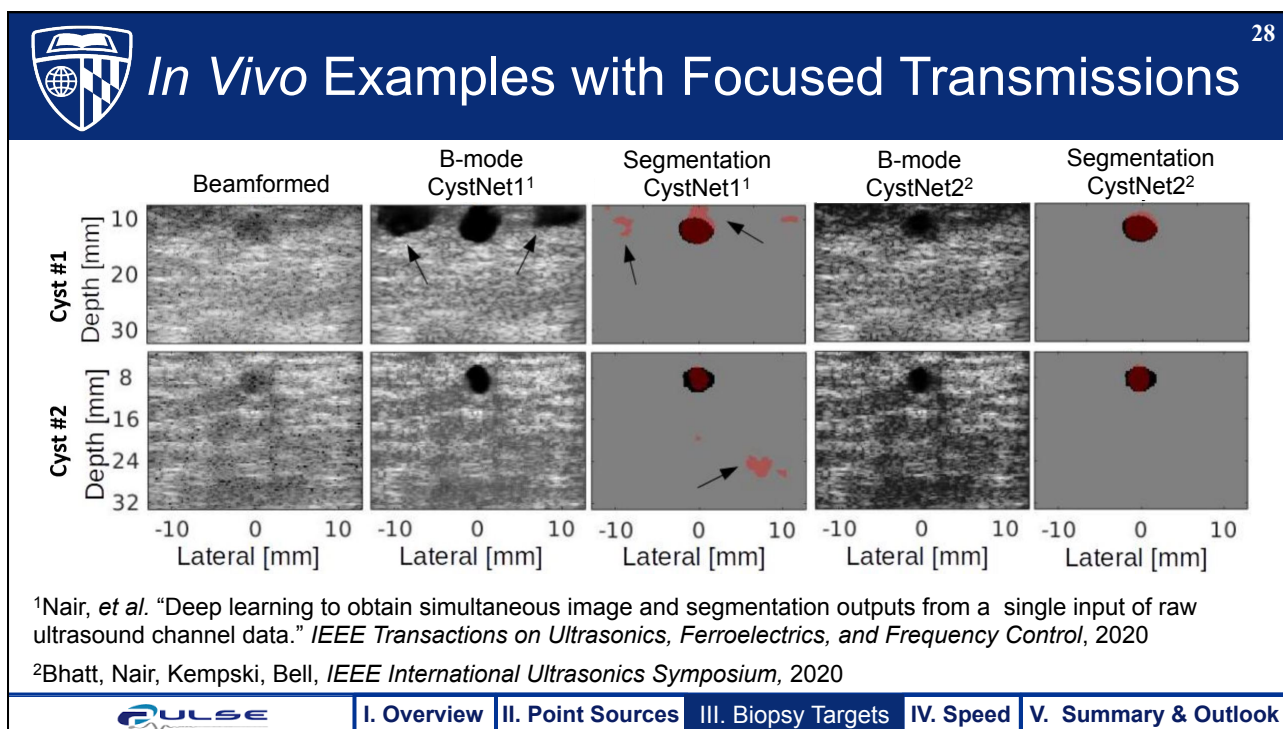
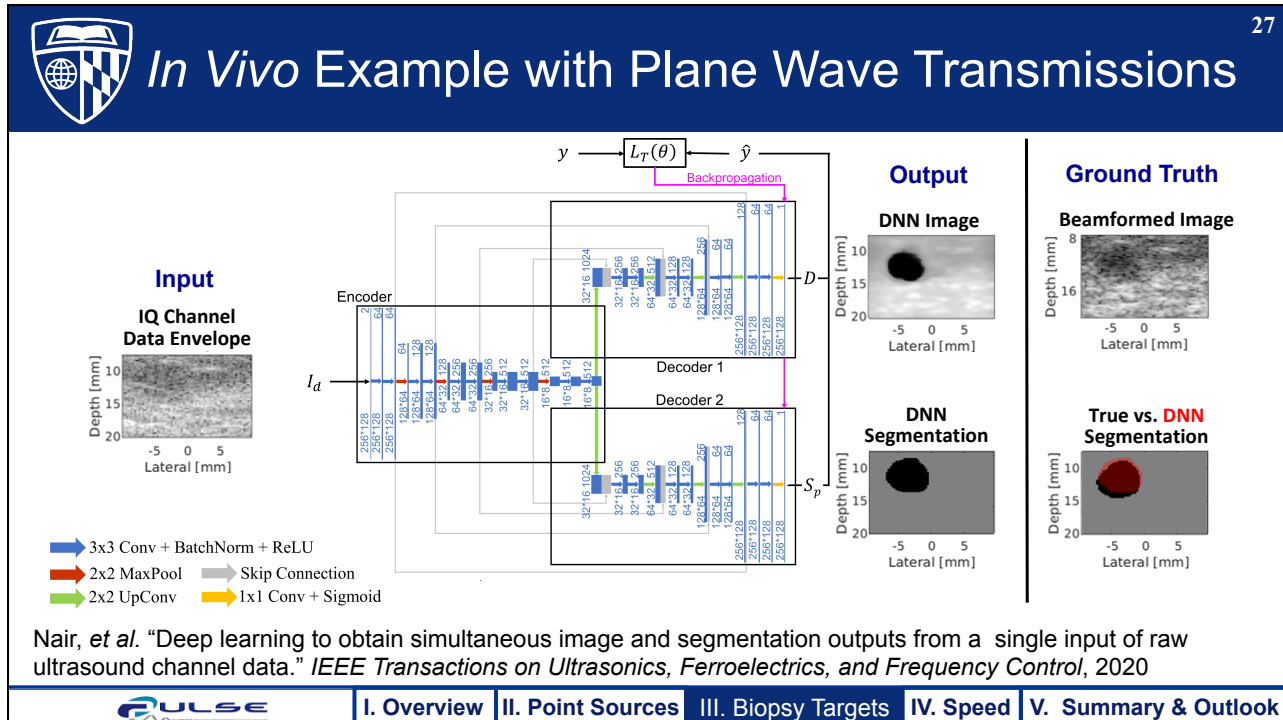
- Network performance degrades in the presence of small cysts
- The radius of each simulated cyst was rounded to the nearest integer mm
- Phantom cysts have similar DSC to simulated cysts of the same size

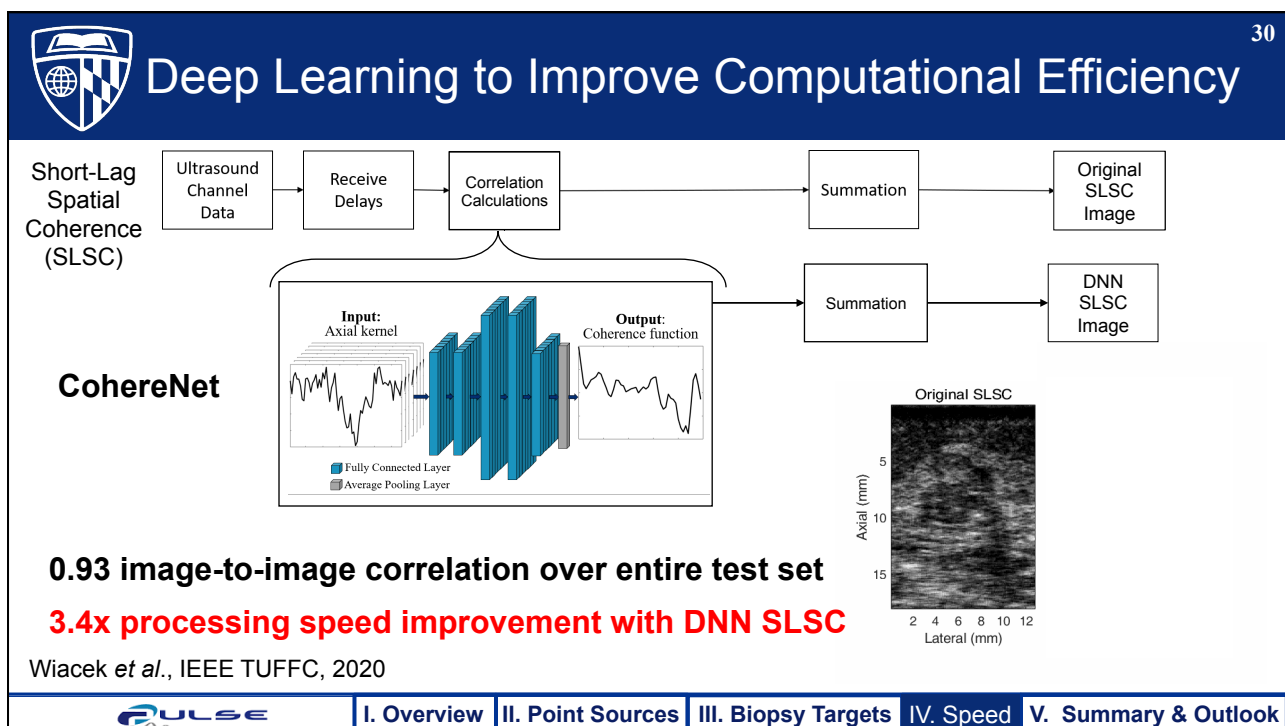
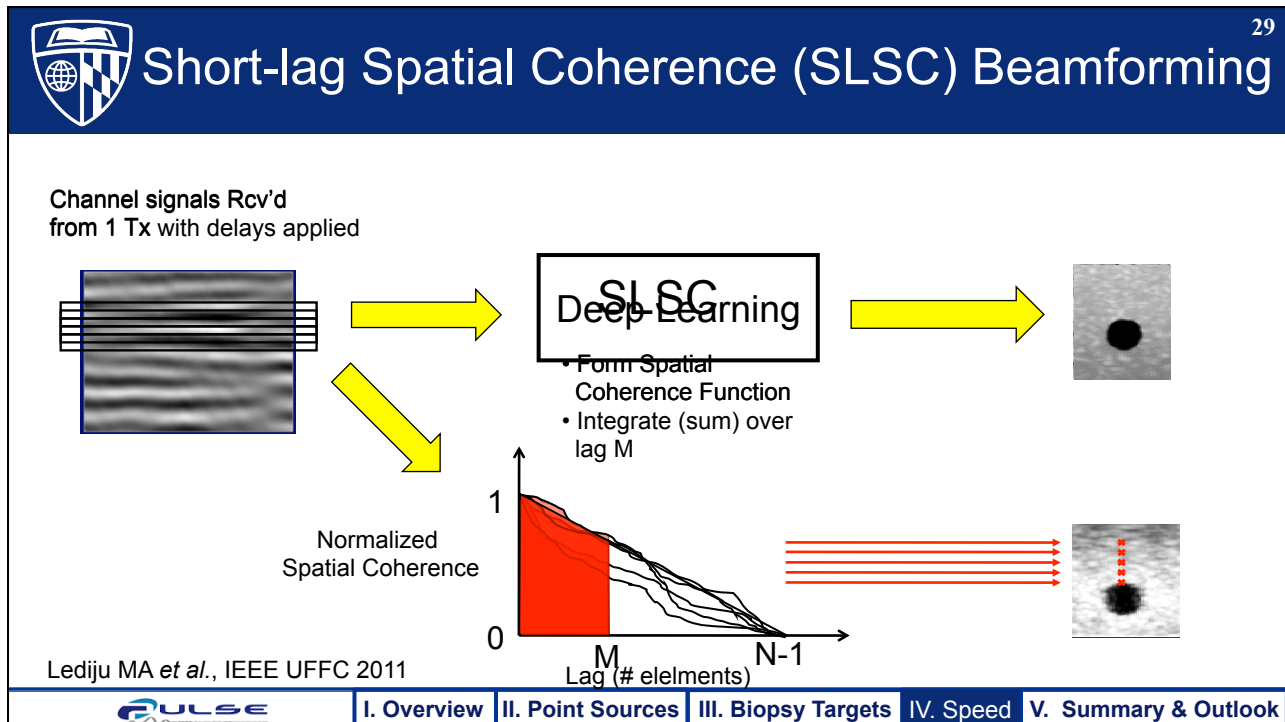


Nair et al. IEEE IUS 2018


[I. Overview](#) [II. Point Sources](#) [III. Biopsy Targets](#) [IV. Speed](#) [V. Summary & Outlook](#)



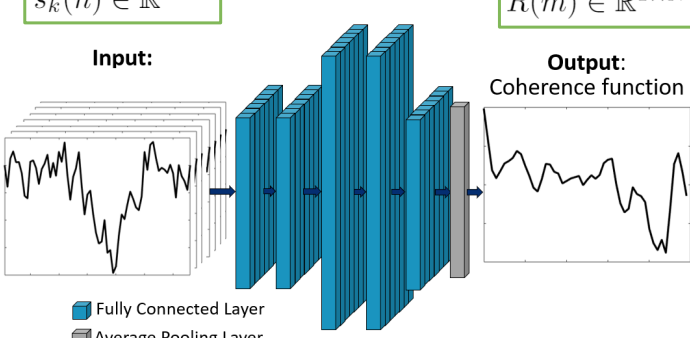




 **CohereNet Architecture** 31

Input: $s_k(n) \in \mathbb{R}^{k \times N}$

Output: $\hat{R}(m) \in \mathbb{R}^{1 \times N}$



Loss Function: $MSE = \frac{1}{m} \sum_{i=1}^m w_i (y_i - \hat{y}_i)^2$

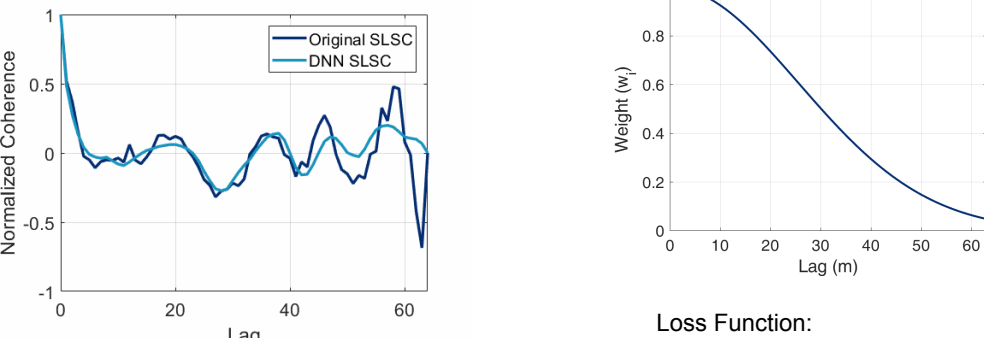
Wiacek et al., IEEE TUFFC, 2020

Layer	Type	Shape	Activation
Input	Input	7 x 64	-
1	FC	7 x 64	ReLU
2	FC	7 x 128	ReLU
3	FC	7 x 128	ReLU
4	FC	7 x 64	Tanh
Output	Avg Pool	1 x 64	-

Hyperparameter	Value
Batch Size	128
Optimizer	adam
Epochs	5

PULSE I. Overview II. Point Sources III. Biopsy Targets IV. Speed V. Summary & Outlook

 **Performance on Test Set** 32



Better performance at shorter spatial lags

Wiacek et al., IEEE TUFFC, 2020

Loss Function: $MSE = \frac{1}{m} \sum_{i=1}^m w_i (y_i - \hat{y}_i)^2$

Gaussian weight with $\mu = 0, \sigma = 25.6$

PULSE I. Overview II. Point Sources III. Biopsy Targets IV. Speed V. Summary & Outlook

 Testing Generalizability 33

- **Data to test network generalizability:**
 - CIRS Model 054GS Phantom Data
 - Alpinion L3-8 Linear Array
 - Alpinion SP1-5 Phased Array
 - Alpinion SC1-6 Curvilinear Array
 - Verasonics P4-2v Phased Array
 - CIRS Model 050 Phantom Data – Alpinion L3-8
 - *In vivo* Liver Data – Alpinion L3-8

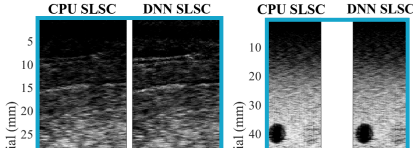
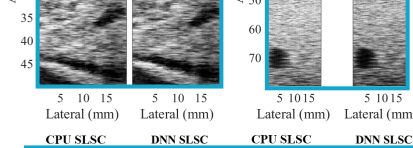


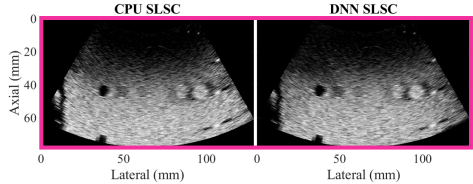


Wiacek et al., IEEE TUFFC, 2020

	I. Overview	II. Point Sources	III. Biopsy Targets	IV. Speed	V. Summary & Outlook
---	-------------	-------------------	---------------------	-----------	----------------------

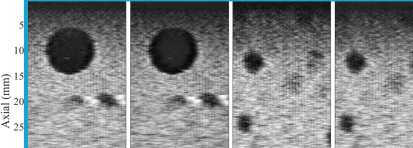
 Network Generalizability 34

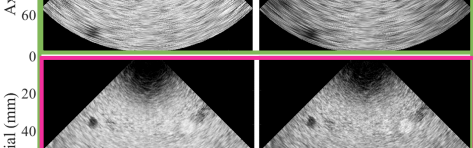





3 transducer geometries

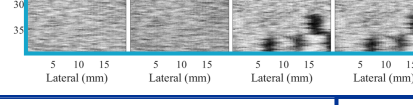
1. Linear
2. Curvilinear
3. Phased

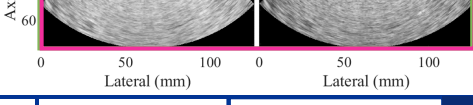




2 ultrasound systems

1. Alpinion
2. Verasonics





3 targets

1. CIRS Model 054GS Phantom
2. CIRS Model 050 Phantom
3. In vivo liver data

0.96 mean correlation between Original SLSC and DNN SLSC images over this entire test set

	I. Overview	II. Point Sources	III. Biopsy Targets	IV. Speed	V. Summary & Outlook
---	-------------	-------------------	---------------------	-----------	----------------------



Summary

35

- US & PA images can be presented in a novel format that extracts information directly from raw channel data with deep learning
- One-step approach to address historical challenges with image quality:

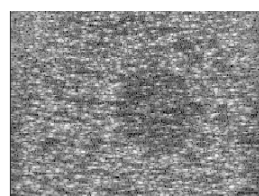
Reflection Artifacts



Segmentation



Speckle & Acoustic Clutter



- Results highlight capabilities of deep learning for image formation and for improving the computational efficiency of advanced beamformers
- Promising for autonomous robotic tracking tasks

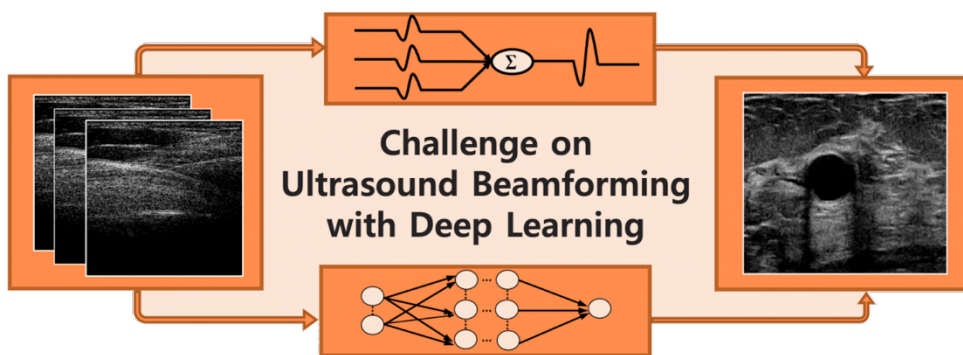


I. Overview | II. Point Sources | III. Biopsy Targets | IV. Speed | VI. Summary & Outlook



Datasets, Code, and Resources

36



Ultrasound Examples: <https://cubdl.jhu.edu/>

Photoacoustic Examples:

<https://github.com/derekallman/Photoacoustic-FasterRCNN>



I. Overview | II. Point Sources | III. Biopsy Targets | IV. Speed | VI. Summary & Outlook

Outlook

37

- Known challenges with deep learning persist
 - Training sets that include multiple possible patient variations
 - Generalizability needed (systems, target size/shape, etc.)
 - Network interpretability
- Evaluation metrics must be tied to specific imaging task
<https://cubdl.jhu.edu/>
- Multiple outputs from single input is highly promising

The diagram shows a curved path of advancement in ultrasound imaging. It starts with 'Spatial Compounding' at the bottom left, followed by 'Harmonic Imaging', 'Elasticity Imaging', 'Doppler Imaging', and 'Coherence-Based Imaging'. At the top right, a red circle represents 'Deep Learning Approach to Beamforming'.

Roadmap of Advances in Ultrasound Imaging

PULSE I. Overview | II. Point Sources | III. Biopsy Targets | IV. Speed | VI. Summary & Outlook

Special Issue of IEEE TUFFC

38

IEEE TRANSACTIONS ON
ULTRASONICS, FERROELECTRICS,
AND FREQUENCY CONTROL

DECEMBER 2020 VOLUME 67 NUMBER 12 (ISSN 1525-8955)

The editorial section features four circular diagrams illustrating deep learning applications in medical ultrasound:

- Motion Estimation:** Shows a flow from raw data to motion fields and then to image reconstruction.
- Segmentation:** Shows a flow from raw data to segmentation masks.
- Elastography:** Shows a flow from raw data to displacement fields and then to elastograms.
- Scatterer Estimation:** Shows a flow from raw data to scatterer parameters and then to image reconstruction.

Deep Learning in Medical Ultrasound—From Image Formation to Image Analysis

Guest Editorial by:

M. Mischi, M.A.L. Bell, R.J.G. van Sloun, Y.C. Eldar

PULSE I. Overview | II. Point Sources | III. Biopsy Targets | IV. Speed | VI. Summary & Outlook



Call to Action

39

Cell

Leading Edge

CellPress

Commentary

Fund Black scientists

Kelly R. Stevens,^{1,*} Kristyn S. Masters,² P.I. Imoukhuede,³ Karmella A. Haynes,⁴ Lori A. Setton,³ Elizabeth Cosgriff-Hernandez,⁵ Muyinatu A. Lediju Bell,⁶ Padmini Rangamani,⁷ Shelly E. Sakiyama-Elbert,⁵ Stacey D. Finley,⁸ Rebecca K. Willits,⁹ Abigail N. Koppes,⁹ Naomi C. Chesler,¹⁰ Karen L. Christman,¹¹ Josephine B. Allen,¹² Joyce Y. Wong,¹³ Hana El-Samad,¹⁴ Tejal A. Desai,¹⁵ and Omolola Eniola-Adefeso^{16,*}

PULSE



Acknowledgements

40

pulselab.jhu.edu

- Graduate Students:

- Derek Allman
- Eduardo González
- Michelle Graham
- Mardava Gubbi
- Kelley Kempski
- Arun Nair
- Theron Palmer
- Joshua Shubert
- Alycen Wiacek
- Ole Marius Hoel Rindal
- Huayu Hou
- Jinxin Dong

- Undergraduate Students:

- Kendra Washington
- Neeraj Gandhi
- Blackberry Eddins
- Margaret Allard
- Brooke Stephanian

- Collaborators:

- Peter Kazanzides, PhD
- Austin Reiter, PhD
- Jonathan Chrispin, MD
- Fabrizio Assisi, MD
- Susan Harvey, MD
- Kelly Fabrega-Foster, MD
- Eniola Falomo, MD
- Kelly Myers, MD
- Lisa Mullen, MD
- George Jallo, MD
- Kaisorn Chaichana, MD
- Jin He, MD
- Kelvin Hong, MD
- Kai Ding, PhD, DABR
- Trac Tran, PhD
- Karen Wang, MD
- Sarah Beck, PhD, DVM

- Senior Research Engineer:

- Anton Deguet

Follow @MuyinatuBell



National Institutes
of Health
NIH Trailblazer Award
NIH K99/R00 EB018994



NSF CAREER Award
ECCS 1751522
NSF EEC 1852155
NSF IIS 2014088



Junior Faculty
Enhancement
Award



JHU Discovery Award



IEEE ULTRASONICS, FERROELECTRICS
AND FREQUENCY CONTROL SOCIETY
Cutting Edge Surgical, Inc.